Functional photonic superstructures: Coherent formation of active-passive photonic band gap heterostructures and photonic subbands

S. M. Sadeghi*
Department of Physics, University of Alabama in Huntsville, Huntsville, Alabama 35899, USA

W. Li
Department of Chemistry and Engineering Physics, University of Wisconsin-Platteville, Platteville, Wisconsin 53818, USA

X. Li and W.-P. Huang
Department of Electrical and Computer Engineering, McMaster University, Hamilton, Canada L8S 4K1
(Received 11 October 2007; revised manuscript received 6 December 2007; published 10 March 2008)

We propose coherently generated photonic heterostructures using a functional photonic superstructure. In the absence of a laser field (control field), such a structure exhibits a conventional passive (off-resonant) photonic band gap. When a region(s) of such a structure is illuminated by the control field, coherent enhancement of refractive index increases the refractive index perturbations of that region, while electromagnetically induced transparency keeps it lossless. This forms a photonic heterostructure consisting of a passive (unilluminated region) and an active (illuminated region) photonic band gap structures. Using such a superstructure, we study a coherently generated photonic quantum well structure wherein two active photonic band gaps sandwich a passive region. We show that, since the active photonic band gaps are roughly twice wider than the passive band gap, they form two photonic barriers around the transparency band located at the longer wavelength side of the passive photonic band gap. This leads to formation of resonant transparency states or photonic subbands, similar to the conduction or valence subbands in electronic quantum well structures. We show that the energies and linewidths of such photonic subbands can be coherently controlled by just adjusting the control field beam.

DOI: 10.1103/PhysRevB.77.125313 PACS number(s): 42.70.Qs, 78.67.De, 42.50.−p

The analogy between photons in spatially periodic dielectric structures and electrons in crystalline semiconductors has led to significant research for fundamental and device applications. These applications include nanodevices, quantum computing, light sources, quantum buffers, etc.[1,2] Significant attempts have been devoted to confine photons in one-, two-, or three-dimensional photonic band gap (PBG) systems, similar to confinement of electrons in quantum wells, wires, or dots. Construction of a photonic quantum dot via patterning a planar optical microcavity structure has already been reported.[3] Here, by decreasing the lateral size of the structure, the optical modes shift to higher energies. These modes are analogous to sharp discrete states of an electronic quantum dot.[4,5] By bringing two or more photonic quantum dots together, as shown in Ref. 6, one can also form a "photonic molecule." The spectroscopy of such a structure has shown that the energy splitting of the confined photonic modes increases with the decreasing the length of the channel joining the two dots, in close analogy to the emergence of electronic bonding and antibonding modes in diatomic molecules. Photonic quantum wells (QWs) have also been studied by sandwiching a medium between photonic barriers formed by several layers of semiconductors. The presence of quantized confined states in such structures, similar to those in semiconductor quantum wells, has been investigated.[7,8]

In the above cases, the photonic potentials responsible for confining photons were generated by spatial variation of semiconductor materials, either by etching or forming a heterostructure of semiconductor materials with different refractive indices. In this paper, we propose formation of photonic barriers using quantum interference and coherence in semiconductors. In other words, we are investigating cases where such barriers are formed by coherent enhancement of refractive index in the presence of electromagnetically induced transparency (EIT). For this purpose, we are studying a *functional* waveguide structure or photonic superstructure that in the absence of a laser field (control field) forms a passive photonic band gap caused by its background refractive index corrugation. Since such a band gap is associated with light scattering along the whole structure with uniform refractive index perturbation [Fig. 1(a)], this structure resembles a bulk semiconductor with an electronic band gap. In other words, the waveguide structure acts as a homogeneous photonic band gap structure. As illustrated schematically in Figs. 1(b) and 1(c), however, when a portion(s) of such a waveguide structure is illuminated by the control field, the refractive index contrast in that region enhances via coherent enhancement of refractive index. This process happens as the control field activates some of the transitions of the QW with wavelengths similar to the Bragg wavelength, making the illuminated region to act as an active PBG structure.[9] As we show in this paper, this sets up a photonic heterostructure associated with the band gap differences between the unilluminated and illuminated regions. We use this property and the fact that the illuminated regions can be easily shifted to any part of the waveguide to demonstrate formation of electromagnetically induced photonic barriers and photonic QWs. As can be seen in Fig. 1, the width of the photonic barrier (L_b) corresponds to the length of the region of the waveguide illuminated by the control field [Fig. 1(b)]. The width of the photonic QW (L_w), on the other hand, corresponds to the length of unilliminated region flanked by two illuminated regions [Fig. 1(c)].

Note that the photonic heterostructures studied in this pa-

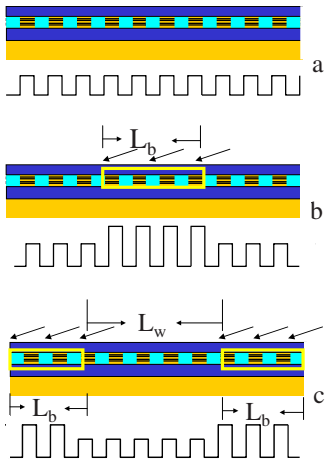

FIG. 1. (Color online) (a) Schematic representation of the functional PBG waveguide structure or photonic superstructure studied in this paper. The parallel lines refer to the corrugated QW regions. The arrows refer to the control field beam illuminating the waveguide structure from the side in one (b) or two locations (c). L_b refers to the length of the illuminated region (barrier), and in (c) L_w represents the width of the photonic QW. In each part, the stepped line refers to the refractive index perturbation along the waveguide.

per have a special resemblance with electronic QW structures. Such QW structures are formed by sandwiching a narrower band gap semiconductor material between two wider band gap semiconductor layers [Fig. 2(a)]. The discrete states (subbands) are formed inside the conduction or valence bands of the narrower band gap (well) semiconductor. The number of these subbands, their energies, and linewidths are determined by the conduction or valence band offsets, which are related to the difference between the electronic gaps of the barriers and the well. They also depend on the width of the middle layer [Fig. 2(a)]. The photonic QW structures investigated here are also composed of a narrower band gap section (passive PBG) and two wider band gap

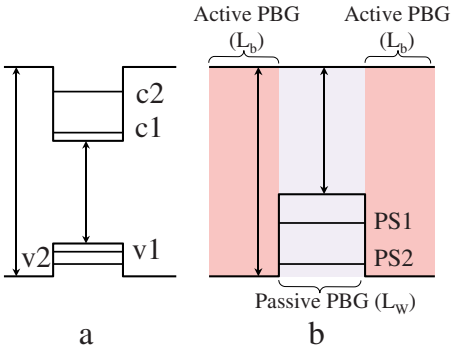

FIG. 2. (Color online) Schematic representations of a single semiconductor QW (a) and photonic QW studied in this paper (b). In (a), c1 and c2 refer to the discrete states inside the conduction band of the narrower band gap layer, and v1 and v2 to those inside the valence band. In (b), PS1 and PS2 refer to the photonic subbands on the longer wavelength transparent side of the passive PBG, corresponding to Fig. 1(c). The doubled-sided arrows represent the electronic (a) or photonic (b) band gaps.

barriers (active photonic PBGs). As shown in Fig. 2(b) and discussed in the following, because of the arrangement of these band gaps, the shorter wavelength edges of these band gaps are nearly aligned. The discrete transparency states (photonic subbands), therefore, are formed in the transparency region at the longer wavelength side of the passive PBG.

Another fundamental issue in this study is the fact that one can adjust the widths of the photonic barriers and quantum wells by just varying the widths of the illuminated regions. Therefore, one can have control over the photonic subbands, their widths, and energies by adjusting the control field beam. Our results show that as the width of the photonic QW reduces, the photonic subband are shifted to the longer wavelength side, toward the edge of the photonic barrier formed by active photonic band gaps. This suggests that the photonic subbands here are, in fact, valencelike, as indicated in Fig. 2(b) (PS1, PS2, etc.). Note that the response time of the system considered in this paper is around picosecond. This allows one to switch off or on the processes discussed here in ultrafast fashion. Therefore, the results of this paper can have applications in various types of optical tunable filters, switches, and laser systems.

Note that, in this paper, we are dealing with coherent nonlinear effects that allow us to optically generate active PBG structures. Active PBGs have also been studied using superradiant excitons, wherein optical coupling between excitons in different QWs led to the band gap.[10] Additionally, tuning of passive PBGs have been investigated using electro- and thermo-optics effects of infiltrated liquid crystals[11] or carrier effects generated by intense laser fields.[12] In such structures, one can also use the strong localization of optical field caused by defects to enhance nonlinear effects in dielectrics and quantum dots [13,14] or to electrically tune the frequency of a defect lasing mode.[15]

Note that the photonic barriers and QWs discussed in this paper are caused by the ability of the functional PBG structure considered here to generate a series of passive and active PBG structures in a single semiconductor chip.[9] Such a structure contains several periods of a semiconductor *n*-doped double QW (DQW) structure [Fig. 3(a), inset] used in a corrugated form in a waveguide structure, as shown in Fig. 1. The QW structure consists of a populated ground subband ($|1\rangle$) and two upper subbands ($|1\rangle$ and $|3\rangle$). When the control laser is off, the 2-3 transitions, which have similar wavelengths as the Bragg wavelength, are not visible to the probe field. Therefore, the structure acts as passive PBG. When the control laser is coherently mixing the 1-3 transitions, however, carriers are excited in $|2\rangle$ and $|3\rangle$, making the 2-3 transition visible to the probe field. Here, however, despite the fact that the electron population in $|2\rangle$ is more than that in $|3\rangle$, EIT makes the 2-3 transitions transparent to the probe field at a narrow frequency range, allowing formation of an active PBG. Since this process happens with enhancement of refractive index of such transitions, as shown schematically in Fig. 1, it can lead to significant increase of refractive index contrast in the illuminated regions without causing any loss.

To discuss these issues quantitatively, we consider the DQW structure consists of 4 and 2 nm $In_{0.5}Ga_{0.5}As$ wells

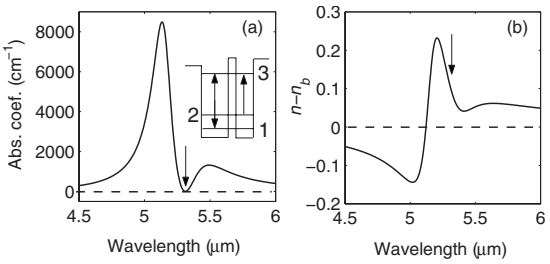

FIG. 3. Absorption coefficient (a) and refractive index (b) of the 2-3 transitions when I_c=0.7 MW/cm^2. The detuning of the control field is considered 4.1 meV. The downward arrow in (a) indicates the wavelength where EIT occurs and that in (b) shows the enhancement of refractive index at the same wavelength. The dashed lines refer to the case when I_c=0. The inset in (a) schematically shows the double QW structure. The energies of the 1-3 and 2-3 transitions in such a structure are, respectively, 391 and 239 meV. The former is coupled by the control field (double-sided arrow), and the latter is detected by the probe field (upward arrow).

separated by 1.5 nm $Al_{0.5}Ga_{0.5}As$ barrier [Fig. 3(a), inset].[9] The left and right barriers are, respectively, $Al_{0.4}Ga_{0.6}As$ and $Al_{0.55}Ga_{0.45}As$. Including the effects of strain and energy-dependent electron effective mass, we find a relatively large dipole moment for the 2-3 transition ($\langle z\rangle_{23}\sim 2.7$ nm) with a transition wavelength of about 5.2 μm. The 1-3 transition occurs at 3.17 μm with $\langle z\rangle_{13}$=0.8 nm. We considered that the electron-electron scattering rate in the ground subband was 4 ps^{-1} and the energy relaxation times of electrons from the third subband to the second and first subbands were, respectively, 2 and 3 ps.[16] In addition, considering the 1-2 transition energy (152 meV) and the carrier density (7×10^{11} cm^{-2}), we assumed that the tunneling time from $|2\rangle$ to $|1\rangle$ was roughly 2.5 ps. The optical response of such a DQW system at the vicinity of the 2-3 transition was calculated using the optical Bloch equations obtained from the following equation:

$$\dot{\rho}^{\mathbf{k}} = -\frac{i}{\hbar}[H+V,\rho^{\mathbf{k}}] + \dot{\rho}^{\mathbf{k}}|_{\text{relax}}. \tag{1}$$

Here, ρ refers to the density matrix of the system, H to its Hamiltonian in the absence of the signal and control fields, and V to the interaction terms of these fields. The second term in the right hand side of Eq. (1) represents the incoherent contributions of the electron-electron and electron-phonon scattering processes. This term contains energy relaxation times, as described above, and polarization dephasing time (γ_{ij}^{-1}). For the latter, based on the parameters mentioned above, we considered γ_{13}^{-1}=0.41, γ_{12}^{-1}=0.45, and γ_{23}^{-1}=1.56 ps. Having the density matrix, we calculated the susceptibility and then absorption and refractive index of the 2-3 transition.

When the control field is off, the 2-3 transition is basically transparent with a refractive index equal to that of the background index of the DQW structure (n_b) (Fig. 3, dashed lines). In the presence of this field, the absorption coefficient and refractive index of this transition can change dramatically. In particular, if we consider that the intensity of this field (I_c) is 0.7 MW/cm^2 and its wavelength is 3.2 μm, as shown in Fig. 3(a), around 5.3 μm an EIT is generated (downward arrow). Considering Fig. 3(b), around the same wavelength, one finds significant enhancement of refractive index. Note that this process is caused by the same resonant coherent processes that generate EIT. Therefore, it is different from the index change caused by carrier effects, liquid crystals, or electric field. EIT and coherent enhancement of refractive index have already been utilized for various applications including coherently induced PBG and laser systems.[9,17,18]

To study coherent generation of photonic QWs and barriers, we consider that the waveguide structure studied here contains 80 periods of the DQW structure etched periodically with 845 nm period. The trenches are then refilled epitaxially with $In_xAl_{1-x}As$. The In content (x) here is adjusted such that the effective refractive indices of these regions (trenches) are less than those of the QW regions in the absence of the control field. The substrate is GaAs and the lower confinement layer is a graded $In_xAl_{1-x}As$ layer, allowing accommodation of high strain and providing the optical confinement needed for the waveguide structure. The upper confinement layer is also taken to be $In_xAl_{1-x}As$ with an average refractive index of 3 in the vicinity of 5 μm, similar to that of the lower confinement layer. The length of total waveguide (L_t) is considered to be 1200 μm and the facets are AR coated. We also assume that the DQWs located a narrow-width ridge illuminated from the side by the control field. This allows us to ignore variation of the control field intensity.[9]

To treat light propagation in the waveguide structure described above, we employed an extended version of the coupled mode theory. In such a theory, we consistently included the strong frequency dependency of both refractive index and absorption at the vicinity of the tranpsarency window (downward arrows in Fig. 3).[9,18] Based on this theory, the electric field along the waveguide can be expressed as

$$E_{\omega_c}^{I_c}(\omega,z) = F_{\omega_c}^{I_c}(\omega,z)e^{-j\beta_0 z} + R_{\omega_c}^{I_c}(\omega,z)e^{j\beta_0 z}. \tag{2}$$

Here, the indices emphasize on the fact here that the optical field propagation along the waveguide is strongly influenced by the intensity (I_c) and frequency (ω_c) of the control field. For the first order corrugation with period Λ considered here, we have $\beta_0=\pi/\Lambda$. $F_{\omega_c}^{I_c}(\omega,z)$ and $R_{\omega_c}^{I_c}(\omega,z)$ refer to the forward and backward waves with frequency ω along the propagation direction (z). To find these functions, we adopt a transfer matrix method, including the effects of the control field:

$$\begin{bmatrix} F_{\omega_c}^{I_c}(\omega,L_t) \\ R_{\omega_c}^{I_c}(\omega,L_t) \end{bmatrix} = T_{\omega_c}^{I_c}(\omega,L_t)\begin{bmatrix} F_{\omega_c}^{I_c}(\omega,0) \\ R_{\omega_c}^{I_c}(\omega,0) \end{bmatrix}. \tag{3}$$

Here, $T_{\omega_c}^{I_c}(\omega,L_t)$ refers to the total transfer matrix. For coherently induced barrier [Fig. 1(b)], this is given by

$$T_{\omega_c}^{I_c}(\omega,L_t) = T(\omega,L)\hat{T}_{\omega_c}^{I_c}(\omega,L_b)T(\omega,L), \tag{4}$$

while for the photonic QW, we have

$$T^{I_c}_{\omega_c}(\omega,L_t) = \hat{T}^{I_c}_{\omega_c}(\omega,L_b)T_p(\omega,L_w)\hat{T}^{I_c}_{\omega_c}(\omega,L_b). \quad (5)$$

Here, $\hat{T}^{I_c}_{\omega_c}(\omega,L_b)$ refers the transfer matrix of the illuminated regions forming the barriers or active PBG. L_w refers to the length of the unilluminated passive region (photonic QW width) when it is flanked by two illuminated regions [Fig. 1(c)]. L_b refers to the width of the region influenced by the control laser, i.e., the barrier width.

$\hat{T}^{I_c}_{\omega_c}(\omega,L_b)$ is given by

$$T^{I_c}_{\omega_c}(\omega,L_b) = \begin{bmatrix} T_{11} & T_{12} \\ T_{21} & T_{21} \end{bmatrix}_{\omega_c,I_c}, \quad (6)$$

where

$$T_{11} = \cosh[\gamma^{I_c}_{\omega_c}(\omega)L_b] + \left(\frac{\alpha}{2} - j\delta\right)\frac{\sinh[\gamma^{I_c}_{\omega_c}(\omega)L_b]}{\gamma^{I_c}_{\omega_c}(\omega)}, \quad (7)$$

$$T_{12} = -j\kappa^{I_c}_{\omega_c}\frac{\sinh[\gamma^{I_c}_{\omega_c}(\omega)L_b]}{\gamma^{I_c}_{\omega_c}(\omega)}, \quad (8)$$

$$T_{21} = j\kappa^{I_c}_{\omega_c}\frac{\sinh[\gamma^{I_c}_{\omega_c}(\omega)L_b]}{\gamma^{I_c}_{\omega_c}(\omega)}, \quad (9)$$

$$T_{22} = \cosh[\gamma^{I_c}_{\omega_c}(\omega)L_b] - \left(\frac{\alpha}{2} - j\delta\right)\frac{\sinh[\gamma^{I_c}_{\omega_c}(\omega)L_b]}{\gamma^{I_c}_{\omega_c}(\omega)}. \quad (10)$$

Here, $\gamma^{I_c}_{\omega_c}(\omega) = \left[\left(\frac{\alpha}{2} - j\delta\right)^2 + (\kappa^{I_c}_{\omega_c})^2\right]^{0.5}$, $\delta = \frac{\omega}{c}n_{\text{eff}} - \beta_0$ in which n_{eff} refers the effective refractive index and $\kappa^{I_c}_{\omega_c}$ is the coupling efficient calculated as reported in Refs. 9 and 18. Note that all these parameters are not only functions of I_c and ω_c, as explicitly shown, but also depend on ω, the signal frequency. α refers to the net modal loss of the system. Transfer functions of the passive parts, i.e., the regions not exposed to the control field, have similar functionalities. However, they are independent of ω, ω_c, and I_c. In addition, their coupling coefficients are real. Note that the parameters used in Eqs. (7)–(10) were obtained by the set of frequency-dependent coupled mode equations describing propagation of light wave in a medium with perturbation of complex susceptibilities.[9]

To start, we consider the case of a photonic barrier, formed by setting up an active PBG at the middle of the photonic superstructure [Fig. 1(b)]. Here, in the absence of the control laser, or when $L_b=0$, the structure acts as a passive PBG with a band gap, as shown in Fig. 4(a). Now, if we assume that the control laser field has the the same intensity and wavelength as those in Fig. 3 ($I_c=0.7$ MW/cm^2 and $\lambda_c=3.2$ μm), illuminating a region with length of L_b, the reflection changes peculiarly. Here, while the shorter wavelength side of the spectrum remains fairly unchanged, the longer wavelength side of the band gap evolves drastically with the increase of L_b. In fact, as this happens, the ripples in the longer wavelength side of the PBG are reduced in number while becoming broad. For $L_b=240$ μm, the number of these

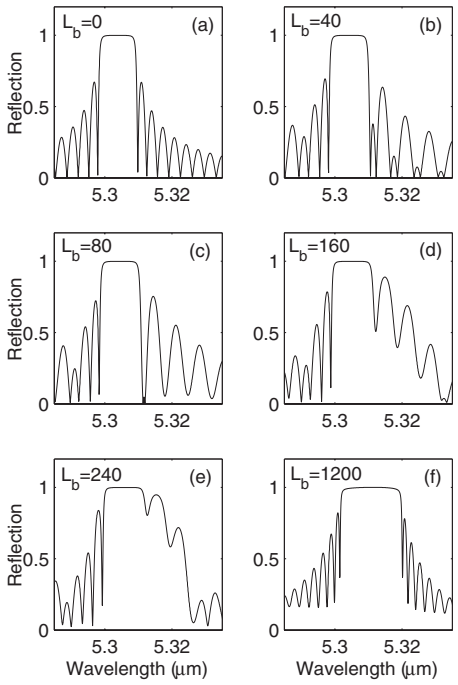

FIG. 4. Variation of the reflection spectra of the waveguide structure when a single central region with different widths (L_b) is illuminated by the control laser field. The intensity and frequency of this laser are considered the same as those in Fig. 2.

ripples reduces to two [Fig. 4(e)]. When L_b is nearly half of the total length of the waveguide ($L_t=1200$ μm), all the ripples are nearly gone and the waveguide acts as a PBG structure with a band gap nearly two times wider than that of the passive PBG (not shown). For larger L_b, the enhanced band gap remains unchanged. When $L_b=1200$ μm, i.e., the laser illuminates the whole structure, the PBG acts again as a homogeneous active photonic structure [Fig. 4(f)]. Note that, in contrast to the passive PBG [Fig. 4(a)], here the probe field is near resonant with the transitions that have relatively large number of electrons in their lower levels and their wavelengths are similar to the Bragg wavelength, i.e., the 2-3 transitions.[9]

The results in Fig. 4 can be qualitatively explained considering how variation of L_b changes reflection spectra of the active and passive regions in the superstructure. As a matter of fact, with the increase of L_b the active part starts to develop a band gap while the reflection of the passive part loses its strength, as it is fragmented into two sections and the length of each section becomes smaller with the increase of L_b. To get some idea about these processes, in Fig. 5(b), we show the reflections of the isolated passive and active regions (homogeneous PBGs) each with 400 μm length. In Fig. 5(a), the whole reflection of the superstructure with $L_b=400$ μm and $L_t=1200$ μm is shown, similar to Fig. 4. Note that in this case since we consider that the illuminated region is centered at the middle of the waveguide [Fig. 1(b)], we have one active region and two passive regions all with the same lengths. Note also that according to Fig. 5(b), for a length of 400 μm, the band gap of the active region is nearly fully formed. This suggests that the reflection seen in Fig.

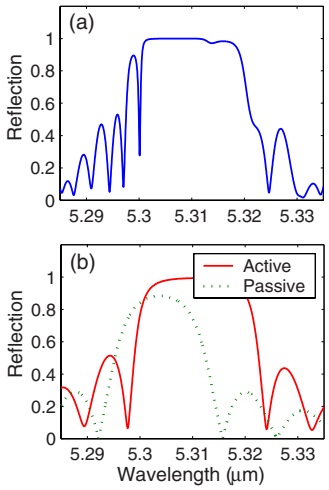

FIG. 5. (Color online) (a) Reflection of the photonic superstructure with the length of active PBG is 400 μm [Fig. 1(b)]. (b) Separate reflections of the active and the passive PBGs each with 400 μm length. Other specifications are the same as those in Fig. 4.

5(a) is mostly dominated by that of the active region. Additionally, in contrast to what we see in Fig. 5(b), the contribution of the passive part in the superstructure [Fig. 5(a)] is expected to have some redshift, as in practice part of its light scattering happens in the active region, which has higher effective refractive index. In a similar manner, since some of the light scattering associated with the active region in this structure happens in the passive parts, the effective refractive index of the active region should be slightly less than the isolated case considered in Fig. 5(b). As a result, in this figure, one should consider a slight redshift (blueshift) for the passive (active) spectrum to have a better description of the events seen in Figs. 5(a) and 4.

In the above cases, we assumed that the control field illuminated the middle of the waveguide structure, forming an active PBG with two passive regions with equal lengths at its sides. An interesting feature of such a structure, however, is that one can shift the position of the active PBG along the waveguide structure. This can be done by steering the laser beam along the waveguide structure, allowing it to illuminate a different location of the waveguide (Fig. 6). Figure 7 represents how the reflection of the photonic superstructure changes as the location of the active PBG (L_b=280 μm) is shifted from the center to the edge. In (a), the active PBG is at the center (L_c=600 μm) and in (d) it is located at the edge (L_c=140 μm). Note that the phenomena seen here can be

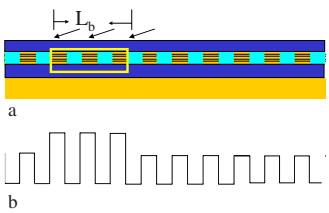

FIG. 6. (Color online) Shift of the photonic barrier (active PBG) via steering of the control field beam.

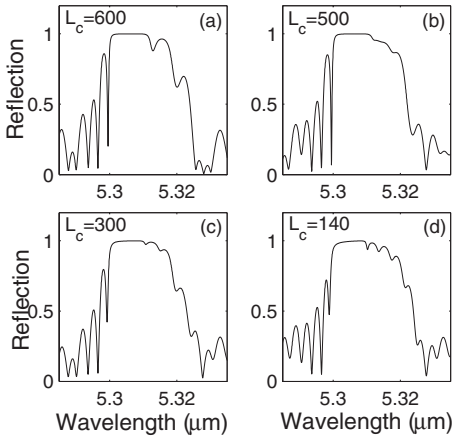

FIG. 7. Variation of the reflection of the waveguide structure when the illuminated region (active PBG) is shifted from the center to the edge (Fig. 6). L_c refers to the distance of the center of the illuminated region (L_b=280 μm) from the left edge. All other specifications are the same as those in Fig. 4.

explained considering the fact that, although the length of the active region remains unchanged, the lengths of the segmented passive sections are changing. In fact, as L_c decreases the length of one of the passive regions increases while the other decreases. In the case of Fig. 7(d), we have one passive PBG with a length of 920 μm and an active region with a 280 μm length.

To generate photonic QW, we consider that the control laser illuminates two regions around the edges of the waveguide, forming two barriers [Fig. 1(c)]. We also consider that the widths of these barriers are same, but similar to the case of Fig. 4 their magnitudes (L_b) are changed by controlling the width of the illuminated regions. The results of calculations are rather unique. As shown in Fig. 8(b), when the width of each barrier is 100 μm, we see a significant change in the longer wavelength side of the band gap. For L_b =200 μm, i.e., L_w=800 μm, we start to see reduction of the number of the ripples while they are becoming quite sharp [Fig. 8(c)]. For wider barriers (narrower QW), we basically see formation of a PBG with enhanced band gap but with some very sharp resonances within [Fig. 8(d)]. The larger L_b becomes, i.e., L_w decreases, the number of these ultrasharp transmission resonances is reduced while they undergo red energy shifting. For L_b=550 μm or L_w=100 μm [Fig. 8(g)], the remaining single resonance approaches the longer wavelength edge of the active PBG.

The results presented in Fig. 8 are analogous to the conduction or valence subbands of a single electronic QW structure [Fig. 2(a)]. In such structures, the number of the quantized states formed within the conduction or valence band of the well depends on its width and the band offset. The transmission resonances seen in Fig. 8 are formed inside the longer wavelength transparent region of the passive region. As one can see, under no condition, any state is formed inside the shorter wavelength region of the band gap, which coincides with the photonic band gap of the unilluminated passive part. The number and energies of such photonic subbands also seem to follow the same rules as the conduction

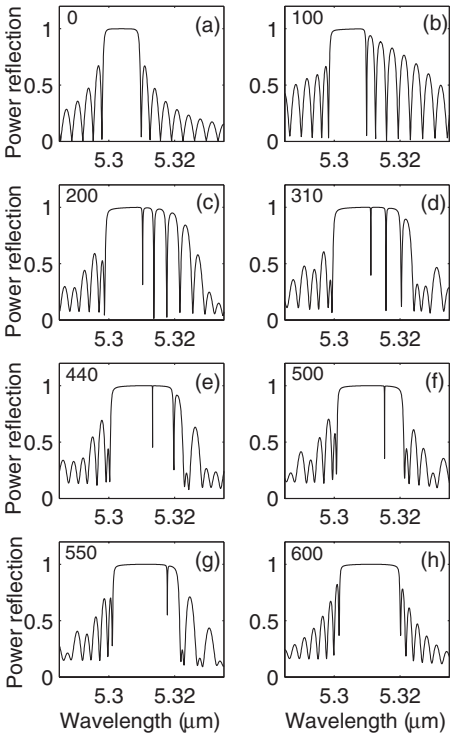

FIG. 8. Reflection of the waveguide structure when two regions of the waveguide are illuminated by the control field [Fig. 1(c)]. The intensity and wavelength of the laser are considered to be similar to those in Fig. 2. The numbers on the left top corners refer to the width of each illuminated region (L_b). The widths of the central unilluminated regions of the waveguide (L_w) are then 1000, 800, 580, 320, 200, 100, and 0 μm in (b)–(h), respectively.

or valence subbands of semiconductor QWs. The redshift of the photonic resonances (subbands) toward longer wavelengths is particularly interesting. Such a shift indicates reaching the band edge of the active PBG as L_w decreases, similar to the semiconductor QWs. This feature suggests that the photonic subbands here are mostly valencelike, as depicted in Fig. 2(b). Regarding the results in Fig. 8, note that enhancement of refractive index in barrier regions causes redshift of the Bragg wavelength, moving the whole PBG toward longer wavelengths. This, however, comes with dramatic enhancement of the band gap. As a result, comparison between Figs. 8(a) and 8(h) shows that the shorter wavelength edges of the passive and active PBGs are not very different. Because of this and the fact that in photonic QW considered here light scattering in the central region is influenced by higher refractive indices in the barrier regions, no significant potential difference between well and barrier regions in shorter wavelength side can be seen here. This feature has been illustrated in Fig. 2(b) as nearly a flatband in the shorter wavelength side.

In conclusion, we proposed that formation of photonic QWs and barriers in a photonic structure consists of a waveguide structure with a uniform corrugation of a multiquantum well structure. The photonic QW and barrier were formed by illumination of the waveguide structure with a laser field, increasing the refractive index perturbation in the illuminated region. This allowed the structure to act as a tandem of two or more passive and active PBGs. Such a process sets up a photonic potential, allowing us to change propagation of the light through the waveguide or form confined photonic states. The former happens when two of such photonic potentials were formed. We showed that by changing the widths of the illuminated regions, we could adjust the width of the photonic QW. This allows us to have control over the widths and energies of the transmission resonances formed in the transparent region on the longer wavelength side of the unilluminated region band gap.

One of the authors (W.L.) gratefully acknowledges financial support from NSF through Grant No. ECS-0555278.

*seyed.sadeghi@uah.edu

[1] C. Santori, D. Fattal, J. Vuckovic, G. S. Solomon, and Y. Yamamoto, Nature (London) **419**, 594 (2002).
[2] O. Painter, R. K. Lee, A. Scherer, A. Yariv, J. D. O'Brien, P. D. Dapkus, and I. Kim, Science **284**, 1819 (1999).
[3] J. P. Reithmaier, M. Rohner, H. Zull, F. Schafer, A. Forchel, P. A. Knipp, and T. L. Reinecke, Phys. Rev. Lett. **78**, 378 (1997).
[4] G. Schedelbeck, W. Wegscheider, M. Bichler, and G. Abstreiter, Nature (London) **278**, 1792 (1997).
[5] U. Banin, Y. Cao, D. Katz, and O. Millol, Nature (London) **400**, 542 (1999).
[6] M. Bayer, T. Gutbrod, J. P. Reithmaier, A. Forchel, T. L. Reinecke, P. A. Knipp, A. A. Dremin, and V. D. Kulakovskii, Phys. Rev. Lett. **81**, 2582 (1998).
[7] J. Zi, J. Wan, and C. Zhang, Appl. Phys. Lett. **73**, 2084 (1998).
[8] Y. Jiang, C. Niu, and D. L. Lin, Phys. Rev. B **59**, 9981 (1999).
[9] S. M. Sadeghi, X. Li, W.-P. Huang, and W. Li, J. Appl. Phys. **101**, 123107 (2007).
[10] M. Hubner, J. P. Prineas, C. Ell, P. Brick, E. S. Lee, G. Khitrova, H. M. Gibbs, and S. W. Koch, Phys. Rev. Lett. **83**, 2841 (1999).
[11] K. Busch and S. John, Phys. Rev. Lett. **83**, 967 (1999).
[12] P. M. Johnson, A. F. Koenderink, and W. L. Vos, Phys. Rev. B **66**, 081102(R) (2002).
[13] E. Lidorikis, K. Busch, Q. Li, C. Chan, and C. Soukoulis, Phys. Rev. B **56**, 15090 (1997).
[14] T. Hattori, Jpn. J. Appl. Phys., Part 1 **41**, 1349 (2002).
[15] R. Ozaki, T. Matsui, M. Ozaki, and K. Yoshino, Appl. Phys. Lett. **82**, 3593 (2003).
[16] J. Faist, F. Capasso, C. Sirtori, D. L. Sivco, J. Baillargeon, A. L. Hutchinson, S.-N. G. Chu, and A. Y. Cho, Appl. Phys. Lett. **68**, 3680 (1996).
[17] S. M. Sadeghi, W. Li, and H. M. van Driel, Phys. Rev. B **69**, 073304 (2004).
[18] S. M. Sadeghi, W. Li, X. Li, and W.-P. Huang, IEEE J. Quantum Electron. **42**, 752 (2006).